

1 SULFATE LEACHING FROM RECYCLED AUTOCLAVED AERATED CONCRETE IN FLOOR
2 SCREEDS IS CONTROLLED BY ETTRINGITE SOLUBILITY

3

4 Jef BERGMANS^a, Peter NIELSEN^a, Ruben SNELLINGS^a, Kris BROOS^a

5 ^aFlemish Institute for Technological Research (VITO), Sustainable Materials Management,
6 Boeretang 200, B-2400 Mol, Belgium,

7

8 Corresponding author: Jef Bergmans (jef.bergmans@vito.be)

9

10 Abstract

11 Autoclaved aerated concrete (AAC) is a lightweight cellular concrete. Recycling AAC in concrete or
12 unbound applications may cause problems because of high amounts of leachable sulfate. This study
13 evaluates the recycling of AAC demolition waste as a replacement of sand in floor screed. The cement
14 binder reacted with sulfate released from the AAC waste to form ettringite. Sulfate release was in line
15 with ettringite solubility control and below leaching limits defined by Dutch environmental legislation.
16 High pH conditions are necessary to avoid excessive sulfate leaching. Pollution of AAC waste with
17 gypsum impurities was found to be detrimental to sulfate immobilisation.

18

19 Highlights

- 20 • Ettringite solubility controls sulfate leaching from products with recycled AAC.
- 21 • High pH conditions secure sulfate immobilisation.
- 22 • Gypsum pollution of recycled AAC is detrimental to sulfate immobilisation.
- 23 • Recycled AAC aggregate can replace 40% of the sand fraction in floor screed.

24

25 Keywords: Autoclaved aerated concrete; sulfate leaching; recycling; immobilisation

26 1 Introduction

27 Autoclaved aerated concrete (AAC) is a lightweight porous building material with a density of
28 400-800 kg/m³ and thermally insulating capacities (0.1-0.2 W/mK) [1,2]. AAC is commonly
29 manufactured using combinations of lime and Portland cement mixed with either finely ground quartz
30 sand or Class F fly ash [1]. These raw materials are mixed with water and aluminium powder, which
31 causes the production of H₂ due to the oxido-reduction of the aluminium powder. This reaction is
32 enhanced by the elevated pH of the cement pore solution. The generation of H₂ gas leads to an overall
33 volume expansion and results in the creation of spherical pores where gas remains trapped inside
34 the cement matrix [2]. This way a highly porous, cellular, material is produced. Calcium sulfate
35 (2-5 wt%), in the form of gypsum or anhydrite, is added to the raw materials to facilitate the formation
36 of more crystalline calcium silicate hydrate phases (particularly tobermorite). This results in higher
37 strength and an end product less susceptible to shrinkage and carbonation [3,4,5].

38 Because of its high porosity and low energy and material consumption [6], AAC can be seen as
39 a sustainable building product. However, the recycling of AAC demolition waste still remains
40 a challenge. AAC aggregate has a lower compressive strength (1-9 MPa) [1] than other stony materials
41 in construction and demolition waste (C&DW). Moreover, the chemical composition of AAC
42 aggregate can cause technical and environmental problems in traditional recycling applications for
43 the stony fraction of C&DW (e.g. the use in foundations). AAC contains an average 12,600 mg/kg dm
44 of leachable sulfate [7], which can lead to technical problems (e.g. efflorescence and internal sulfate
45 attack) in building materials [8,9,10] and ecotoxicological effects (salinity, sulfide formation,
46 eutrophication) caused by leaching in groundwater [11].

47 Since AAC demolition waste cannot be recycled in the applications that are used for the stony
48 fraction of C&DW (mostly unbound foundations), it is labelled as a “problem fraction” by the Waste
49 Agency of Flanders OVAM. Currently, it is possible to use AAC aggregate as a replacement for
50 the sand fraction in the production of new AAC. However, this replacement is generally limited to
51 20% of the sand fraction and to the use of AAC production and construction waste. AAC demolition

52 waste can contain impurities, resulting in visual contaminations and problems in the AAC production
53 process [12].

54 Zaetang et al. (2013) investigated the use of AAC as a lightweight aggregate in pervious concrete.
55 The use of AAC aggregate strongly reduced (3-4 times) the density and thermal conductivity
56 compared with pervious concrete produced with natural aggregates [13]. The effects of sulfate
57 leaching were not investigated.

58 Schoon et al. (2013) investigated the use of AAC waste as an alternative raw material for Portland
59 clinker production. Use in this application was possible, but showed several difficulties (e.g. bound
60 H₂O, SiO₂ content and milling costs, impurities) [14]. In the study of Karczmarczyk et al. (2014) [15],
61 AAC aggregate (1-6 mm) was tested as a green roof substrate. The high water absorption and P-
62 removal capacity of AAC aggregate and its removal efficiency in low phosphorus concentrations
63 make it an interesting material for this application. However, AAC aggregate has a negative impact on
64 the water environment because of its sulfate release. Other recycling options for AAC waste include
65 the use of AAC aggregate as oil absorbent or (low-grade) filler for cat litter boxes [12].

66 To create sufficient viable recycling routes for AAC waste, the problem of sulfate leaching needs to
67 be solved, for instance by immobilisation of the leachable sulfate by chemical binding in cement
68 hydration products. Brouwer et al. (2000) described a method for chemically immobilizing sulfate
69 from screening sands, which contain up to 6 wt% sulfate, by the use of Portland cement [16]. In this
70 approach the sulfate is captured by reaction with 3CaO.Al₂O₃ (C₃A) from the cement to form
71 ettringite. The C₃A content in Portland cements is limited to a few percent (3-8 wt%), and sulfates in
72 the form of gypsum or anhydrite are already added to control the setting of the cement. Therefore,
73 the uptake potential of additional sulfate by regular Portland cement is rather limited. In addition, too
74 high dosages of sulfate (oversulfation) effectively delay the hydration of the clinker phases and thus
75 the strength development [17,18,19].

76

77 As an alternative, Ambroise and Péra (2004, 2008) treated demolition waste containing calcium
78 sulfate by means of calcium sulfo-aluminate (CSA) clinker. Here, depending on the initial sulfate
79 dosage of the cement, a much higher uptake potential can be achieved by reaction with the main
80 ye'elinite $[\text{Ca}_4(\text{AlO}_2)_6\text{SO}_4]$ component. They showed that calcium sulfate was entirely consumed
81 when the ratio of CSA to calcium sulfate was 4:1 or higher [20,21].

82 Sulfate dosing into CSA or calcium aluminate cements (CAC) is commonly used to control setting
83 and effect volume expansion [22,23]. However, too high gypsum contents lead to uncontrolled volume
84 expansion, cracking and failing of the hardened cement. This is likely controlled by the build-up of
85 crystallisation pressure by ettringite in micropores [24]. Overall, at present sulfate levels in
86 cementitious materials are being closely monitored and maximum levels are in place to avoid negative
87 effects such as slow hardening, dimensional instability or cracking. In the future, product design and
88 manufacturing will also need to take into account after-life reuse and recycling opportunities. Meeting
89 environmental regulations will be one of the prime requirements to enable high-value recycling
90 opportunities.

91 In this respect, this paper evaluates the recycling of AAC as fine aggregate (0-8 mm) in floor
92 screed formulations made of Portland and blended cements in view of the Dutch sulfate leaching
93 regulations [25]. This application was chosen because of low compressive strength requirements.
94 Sulfate immobilisation mechanisms are described and used to establish product boundary conditions.

95 **2 Materials and methods**

96 **2.1 Phase composition of AAC**

97 The mineralogy of the AAC samples was examined by X-ray powder diffraction (XRD) analysis
98 using a Philips X'Pert Pro diffractometer, equipped with a Cu anode X-ray tube operated at 40 kV and
99 35 mA and using an automatic divergence slit. Specimens were scanned from 2 to 120° (2θ), with
100 a step size of 0.04° and a dwell time of 4 seconds per step.

101 **2.2 Floor screed formulations with AAC waste**

102 First, AAC was crushed with a disk mill to below 8 mm. Second, floor screed mixtures were
103 produced with AAC aggregate (0-8 mm, 530 kg/m³) and C&DW mixed recycled aggregates (0-8 mm,
104 800 kg/m³, produced by an industrial C&DW crushing installation), using different types of cement
105 (CEM I, CEM II, CEM III; 140 kg/m³). Tap water (280 l/m³) was added and the materials were mixed
106 in a concrete mixer. The mixtures were poured in cylindrical moulds (h = 12 cm, d= 10 cm),
107 unmoulded after 24 h and further cured for 28 days at 20 °C, 100% relative humidity before further
108 testing.

109 The mechanisms of sulfate immobilisation (e.g. pH dependency) in the floor screed formulations
110 were studied on samples with pure AAC aggregate. In a second stage, to study the effect of gypsum
111 contamination, formulations were prepared with aggregates from crushed AAC demolition waste.

112 **2.3 Total sulfur**

113 The total sulfur content of the floor screeds was analysed with inductively coupled plasma atomic
114 emission spectroscopy (ICP-AES) (ISO 11885) after crushing (<100 µm) and closed microwave
115 digestion with HCl/HNO₃/HF/H₃BO₃.

116 **2.4 Sulfate leaching**

117 The leaching of sulfate from the AAC aggregate, mixed recycled aggregates and cement stabilized
118 sand products was analysed using batch leaching tests. The European EN 12457-2:2002 compliance
119 test for leaching of granular waste materials and sludges was carried out.

120 The materials (<4 mm) were brought in contact with the leaching liquid (deionized water,
121 L/S = 10) with the aid of an overhead mixer (5 turns/min.). This method is based on the assumption
122 that a state of equilibrium (or near-equilibrium) is reached between the liquid and the solid phases
123 during the test period (24 h). After 24 h, the solid residue was separated from the liquid by filtration
124 (size filter pores: 0.45 µm). The pH of the leaching liquid was measured immediately after filtration.
125 The sulfate concentration of the leaching liquid was measured by liquid chromatography and
126 conductivity detection (ISO 10304-1:2007).

127 **2.5 Speciation-solubility modelling**

128 In a first stage, speciation-solubility modelling was carried out using Visual MINTEQ 3.1, using
129 updated and expanded data from the NIST Critical Stability Constants database, to determine
130 the solubility of ettringite as a function of pH. In the model, ettringite was assumed to be the infinite
131 solid phase. Diaspore and gypsum were added to the calculations as possible precipitation products.
132 The pH was varied between 10.5 and 12.5. The ionic strength of the solution was calculated from
133 the elements in solution.

134 In a second stage, the fate of sulfate released from the AAC by (partial) reaction with or leaching to
135 the cement matrix was modelled. Thermodynamic modelling of the cement hydrate assemblage was
136 carried out using the Gibbs free energy minimization programme GEMS v3.2. GEMS calculates
137 the equilibrium phase assemblage and solution speciation at the defined input composition.
138 The thermodynamic database used was the PSI/Nagra 12/07 general database for aqueous species and
139 common solids [26]. This was supplemented with the cemdata14 database for cement
140 hydrates [27,28]. The effect of sulfate on the cement hydrate assemblage and pore solution
141 composition and the sulfate uptake threshold was evaluated for CEM I floor screed formulations.
142 The Portland cement was taken to be fully hydrated. Averaged literature compositions for Portland
143 cement and AAC waste were adopted [14,29].

144 **2.6 Electron microscopy**

145 The microstructure of the floor screed products was investigated by electron microscopy.
146 Representative samples were cut from the centre of the hardened floor screed specimens and vacuum-
147 impregnated using a low-viscosity epoxy resin. Polished sections of the impregnated samples were
148 prepared by gradually polishing the exposed sample surface down to 1 μm diamond grit size. A water-
149 free polishing lubricant was used to avoid artificial reactions with the freshly exposed surface.
150 The polished sections were Pt-coated preceding microscopic analysis. A FEI Nova NanoSEM 450
151 electron microscope equipped with field emission gun was operated at 15 kV acceleration voltages.
152 Images were acquired in backscattered electron mode at a working distance of 6.2 mm.

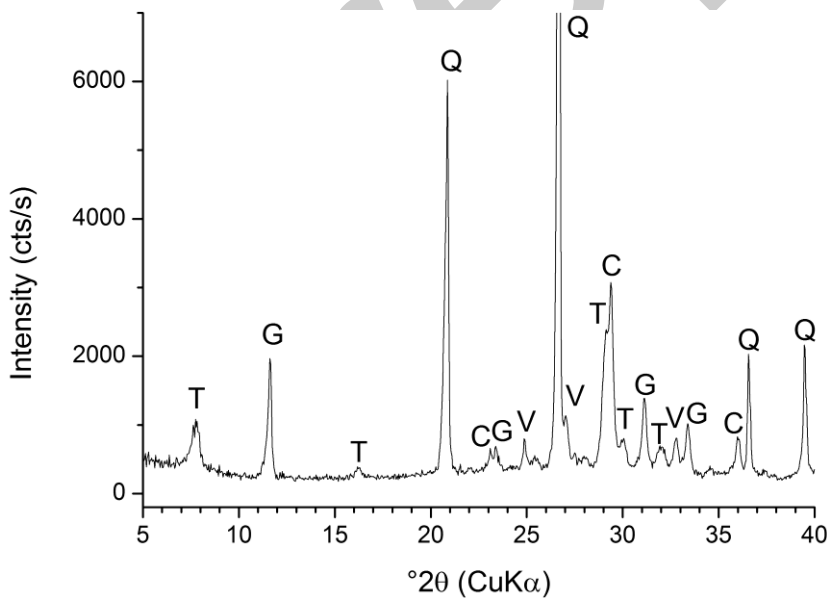
153 Energy dispersive spectroscopy (EDS) point analyses and multispectral element mappings were
154 acquired in order to study the impact of gypsum addition on the binder chemistry. Specific attention
155 was paid to the distribution of sulfur in the cement matrix.

156 3 Results and discussion

157 3.1 Raw material characterisation

158 The phase composition of AAC demolition waste was measured by XRD (Figure 1). The AAC
159 aggregate mainly contains quartz [SiO_2], 11Å-tobermorite [$\text{Ca}_5\text{Si}_6\text{O}_{16}(\text{OH})_2 \cdot 4\text{H}_2\text{O}$], calcite [CaCO_3],
160 vaterite [CaCO_3] and gypsum [$\text{CaSO}_4 \cdot 2\text{H}_2\text{O}$]. No crystalline calcium-aluminate hydrate phases
161 (e.g. ettringite, AFm phases) were found. The average chemical composition for AAC production
162 waste from the Flemish AAC factory (Xella) is given in Table 1 [14]. Xella represents more than 90%
163 of the Flemish market. Table 1 also gives the typical Portland cement compositions used in
164 the thermodynamic modelling of the cement hydrate assemblages. It is important to note that the AAC
165 shows higher SO_3 and lower Al_2O_3 content when compared to Portland cement. This results in
166 the presence of unbound gypsum in the AAC matrix and renders the material liable to sulfate leaching.

167



168

169 Figure 1. XRD pattern of the AAC aggregate from demolition waste. The main reflections are assigned to
170 tobermorite (T), gypsum (G), quartz (Q), vaterite (V) and calcite (C).

171 Table 1. Chemical composition of the AAC aggregate (average of production waste, Schoon et al. [14]) and
 172 Portland cement (averaged compositions used in thermodynamic modelling [29])

Oxide	AAC	Portland cement
	wt. %	
SiO ₂	53.90	19.51
Al ₂ O ₃	1.93	5.37
Fe ₂ O ₃	0.68	2.96
CaO	28.47	63.15
MgO	0.36	1.57
K ₂ O	0.48	1.00
Na ₂ O	0.20	0.25
SO ₃	2.10	4.13
TiO ₂	0.08	0.26
P ₂ O ₅	0.10	0.14
CO ₂	3.29	0.54

173
 174 The leaching of sulfate by dissolution of soluble gypsum is investigated by sulfate leaching testing.
 175 Sulfate concentrations in the leachates of the pure AAC aggregate and the mixed recycled aggregates
 176 were 11,000 and 2,400 mg/kg dm, respectively. For both materials this is above the Dutch limit value
 177 of 1,730 mg/kg dm, which prevents direct reuse. Table 2 compares these leaching values to literature
 178 reports [7,30,31]. The results here are in line with previous tests obtained by similar experimental
 179 procedures.

180

181 Table 2. Sulfate leaching of the raw materials and comparison with literature data.

Material	pH	Sulfate leaching	Sulfate leaching	Reference
		sample (mg/kg dm)	literature (mg/kg dm)	
AAC aggregate	11.6	11,000	12,600	Lang-Beddoe & Schober (1999) [7]
Mixed recycled aggregates	9.3	2,400	1,040	OVAM (2006) [30]
			390-4,700	Vrancken & Laethem (2000) [31]

182

183 **3.2 Sulfate leaching of the floor screed products**

184 **3.2.1 Sulfate leaching and pH**

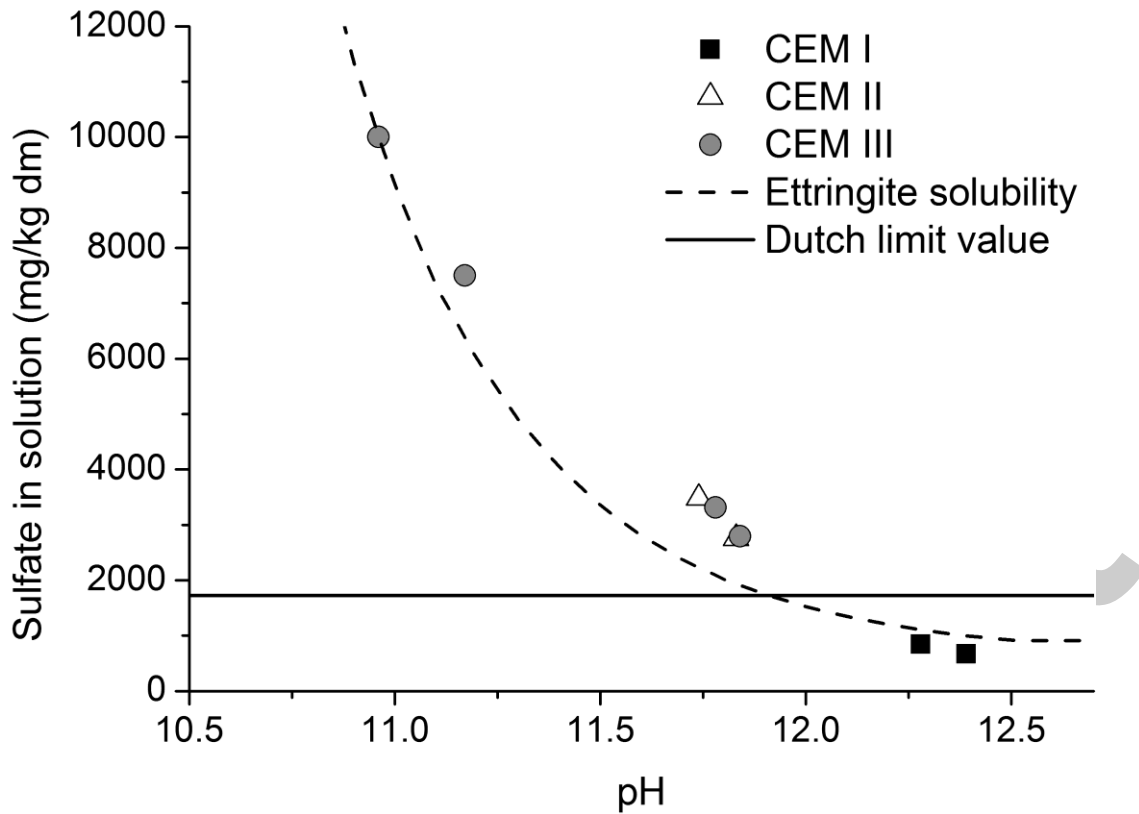
185 The results of the batch leaching tests on the floor screed samples with pure AAC aggregate are
 186 shown in Figure 2. Clearly, sulfate leaching increased with decreasing leachate pH over the pH range
 187 of 12.5 to 10.5. This pH dependency of sulfate leaching is in line with the modelled ettringite
 188 solubility (Fig. 2). A second observation is that floor screeds made of blended cements (CEM II,
 189 CEM III) are less resistant to sulfate leaching. Apparently, the blended cements show a lower pH
 190 buffering capacity than CEM I Portland cement and a lower leaching solution pH is established over
 191 the duration of the leaching test.

192 The observation that formulations containing blended cements are less resistant to sulfate leaching
 193 can be explained by the occurrence of a pozzolanic reaction in the blended cements. The pozzolanic
 194 reaction of fly ash and slag may consume readily accessible Ca(OH)_2 and thus partially deplete
 195 the alkalinity of the cement. However, comparison to other experimental studies on blended cement
 196 hydration [32,33] learns that it is improbable that all portlandite in the system is consumed over
 197 the relatively short times of hydration experienced by the floor screed products (7 days). Similarly,
 198 if portlandite would still be present in the system, thermodynamic calculations indicate that a pH of
 199 around 12.4 should be established in the leaching solutions.

200 The observed low pH indicates that the establishment of a thermodynamic equilibrium may be
201 kinetically hindered or affected by ongoing reactions such as the pozzolanic reaction. Matschei and
202 Glasser (2011) [34] investigated cement hydrate equilibration times in water and concluded that for
203 a substance to act as a buffer it should be available in sufficient quantity and at high reactivity
204 (e.g. high exposed surface area to the solution) and should dissolve sufficiently fast to quickly reach
205 equilibrium. In case of portlandite, dissolution was found to be sufficiently fast to reach equilibrium
206 over a time span of a few minutes [34].

207 Therefore, the low pH encountered in the leaching solutions of the blended cement products cannot be
208 explained by slow portlandite dissolution. Rather, high pH and portlandite saturation may not be
209 reached because of occlusion of portlandite by surrounding pozzolanic reaction products (reduction of
210 reactive surface area), combined with an ongoing pozzolanic reaction during leaching (competitive
211 reaction). The latter effect is common in blended cements, portlandite undersaturation and a reduction
212 in alkalinity are common features [29,32]. Moreover, the evaluation of portlandite saturation in
213 a solution contacted with a hydrating cement lies at the base of the EN 196-5 pozzolanicity test
214 (Frattoni test), where undersaturation is used to diagnose the occurrence of a pozzolanic reaction.

215



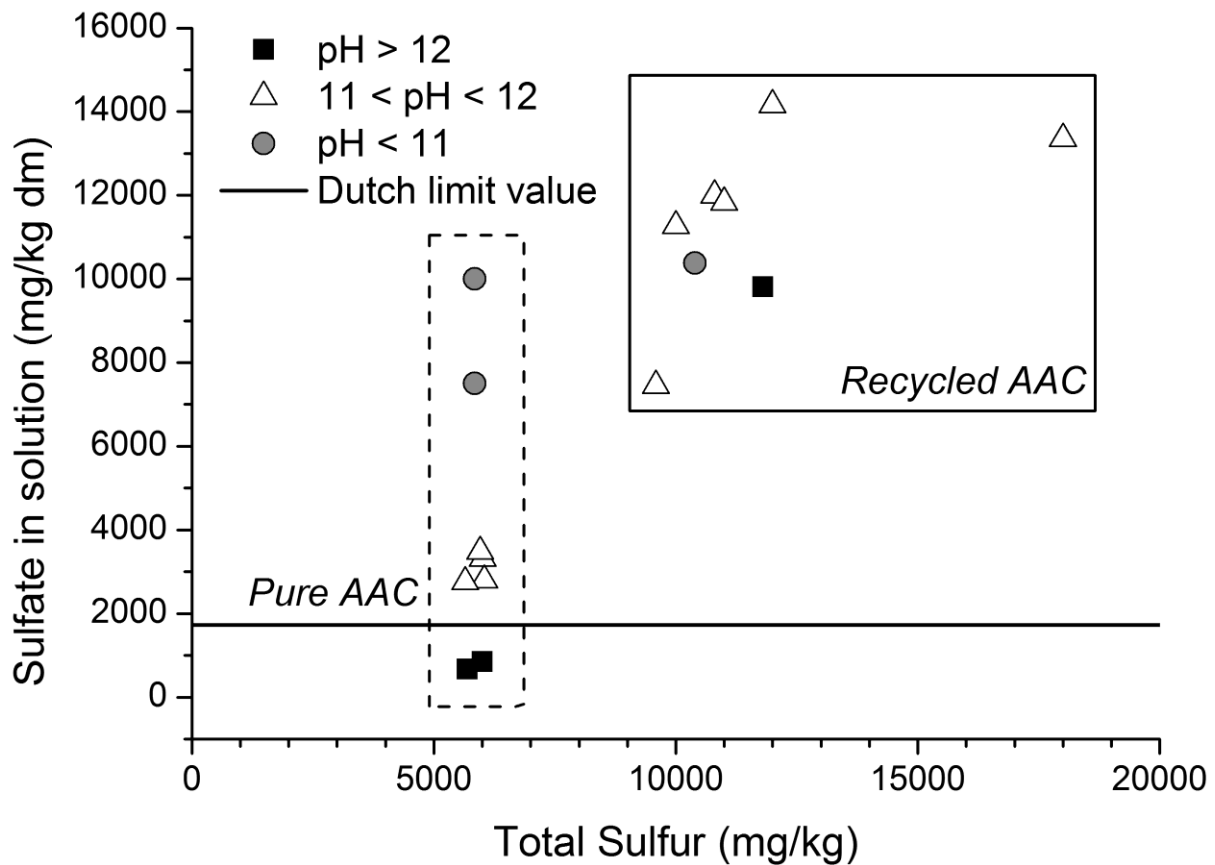
216

217 Figure 2. Sulfate leaching of floor screed products (curing: 7 days) with pure AAC aggregate as a function of
 218 the pH of the leachate (L/S = 10).

219 3.2.2 Effect of gypsum contamination on sulfate leaching

220 In a second phase, AAC aggregate from demolition waste, containing gypsum contamination, was
 221 used for the production of floor screed products. Figure 3 shows sulfate leaching as a function of total
 222 sulfur content of the floor screed products (both with pure AAC aggregate and AAC aggregate from
 223 demolition waste). It is inferred that in the present formulation, floor screed products having high total
 224 sulfur contents experience strong sulfate leaching. This means that in case gypsum contaminated AAC
 225 aggregate is used, the total sulfur content of the system increases significantly and the immobilisation
 226 capacity by ettringite formation can become exhausted. Superimposed on the pH effect, there appears
 227 to be a total sulfur threshold beyond which sulfate can no longer be bound by formation of ettringite.

228



229

230 Figure 3. Sulfate leaching of the floor screed products (curing: 28 days) as a function of the total sulfur content.

231 The leachate results are subdivided by solution pH.

232

233 Thermodynamic modelling of sulfate uptake by a CEM I based floor screed supports the concept of
 234 a sulfate uptake threshold that should not be exceeded. Figure 4 gives the modelled Ca and sulfate
 235 concentrations in the leachate as a function of the reactive gypsum present in the AAC waste for a
 236 CEM I based floor screed.

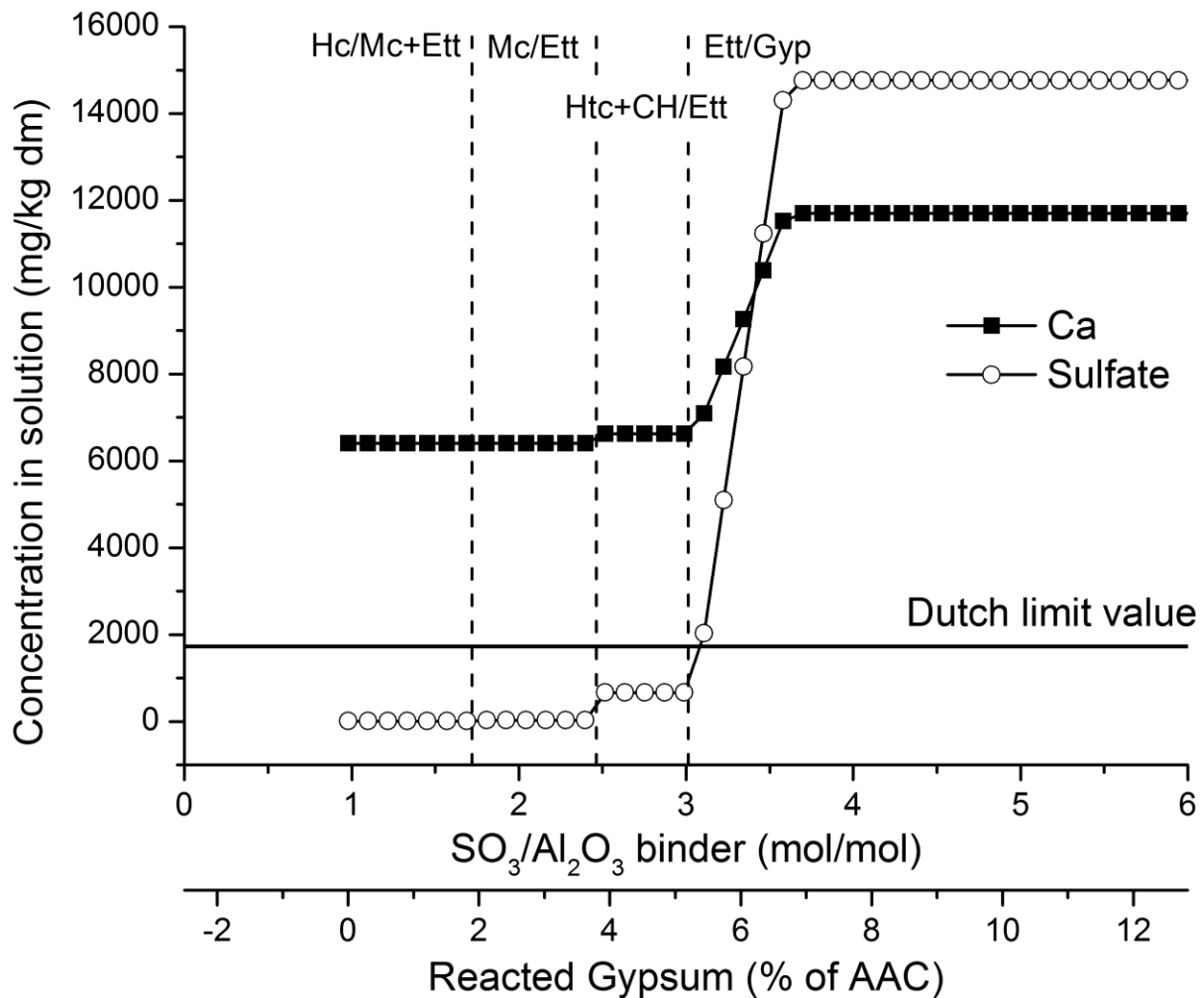
237 The modelling predicts sulfate leaching to comply with the limit value as long as reactive
 238 gypsum/sulfate can be converted into ettringite by reaction with hemihydrate, monocarbonate or
 239 hydrotalcite phases. In case excess reactive gypsum/sulfate is present, sulfate concentrations in the
 240 leachate are predicted to increase steeply and exceed the limit value. Since gypsum equilibrates
 241 relatively fast (few minutes) with a leaching solution [34], it will control sulfate concentrations
 242 through its solubility product. This is consistent with our experimental observations that suggest
 243 noncompliant sulfate leaching in the presence of excess gypsum.

244 Thus, to enable the reuse of AAC waste in cementitious products it is crucial to avoid the intake of
245 gypsum during recycling. In addition, reducing the free gypsum level in the AAC product itself will
246 lower the risk of exceeding the sulfate uptake threshold. A maximum total sulfur content of the
247 product, $S_{tot,max}$ [mg/kg dm], for compliance with sulfate leaching regulations can be calculated by
248 mass balance, assuming that 1) all sulfur reacts with the binder, and 2) Al-ettringite is the ultimate
249 cement hydrate sulfate sink, as:

$$S_{tot,max} [mg/kg dm] = 9435 X_{bind} ((Al_2O_3)_{bind} [wt\%])$$

250 where X_{bind} corresponds to the weight fraction of the cement binder in the final product, and $(Al_2O_3)_{bind}$
251 identifies with the Al_2O_3 content in wt.% of the cement binder. Since some of the sulfur will be taken
252 up into the C-S-H cement hydrate [34], the actual sulfate uptake limit will be somewhat higher.
253 However, equation 1 is useful and can serve as a first, safe indication of maximal sulfur levels for
254 recycled products.

255



256

257 Figure 4. Modelled effect of reactive gypsum and sulfate additions on Ca and sulfate concentrations in the
 258 leachate of a CEMI floor screed product (L/S = 10). No distinction is made between gypsum from the AAC itself
 259 or from contaminations included during recycling. Thermodynamic equilibrium is assumed and sulfate
 260 concentrations are controlled by binder chemistry and the respective hydrate buffering pairs:
 261 hemicarbonate/monocarbonate + ettringite (Hc/Mc+Ettringite), monocarbonate/ettringite (Mc/Ettringite), hydrotalcite +
 262 portlandite/ettringite (Htc+CH/Ettringite), ettringite/gypsum (Ettringite/Gypsum). The Dutch leaching limit value is exceeded
 263 once extra gypsum can no longer be bound into ettringite.

264 **3.3 Microstructure**

265 The microstructure of floor screeds with and without gypsum contamination was investigated by
 266 electron microscopy. Given the high amount of aggregates in the floor screeds, microanalysis of the
 267 chemistry selected areas by EDS was preferable over bulk characterization techniques such as XRD.

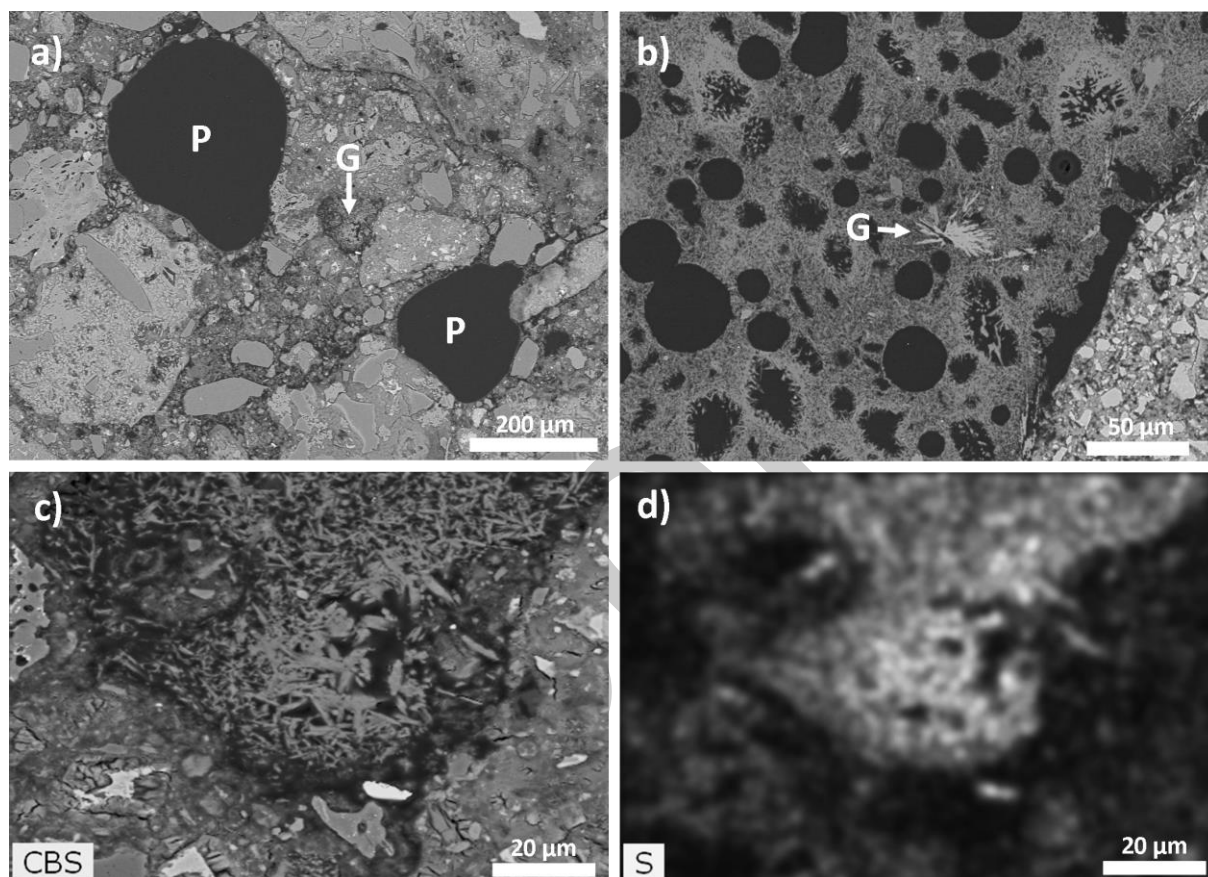
268 Figures 5a-c show a selection of representative backscattered electron images of floor screeds
269 contaminated with gypsum particles. Gypsum aggregate particles were clearly observed as porous
270 aggregates of elongated gypsum crystals (Fig 5c). The outer rim of the gypsum grains was often
271 observed to be very porous and ill-defined. The latter features are indicative for an interfacial reaction
272 between the gypsum and the cement. On the other hand the core of the gypsum particles appears
273 undisturbed and high in S (Fig. 5d). The persistence of gypsum in floor screed samples hydrated for
274 28 days indicates that gypsum is stable and that the Al_2O_3 reservoir of the cement is depleted,
275 as supported by excessive levels of sulfate in the leachate solutions of the corresponding samples
276 (Figure 3).

277 Contrary to gypsum particles in direct contact with the cement matrix, the gypsum contained in the
278 AAC particles do not show signs of reaction (Fig. 5b). Enclosure within the AAC aggregate particles
279 drastically reduces the available reactive surface area and exposure to the cement pore solution.
280 Moreover, if contamination of the AAC waste by external gypsum sources (e.g. plaster boards) is
281 excluded, than the rather small amounts of gypsum in the AAC itself can be easily contained by
282 reaction with the Portland cement.

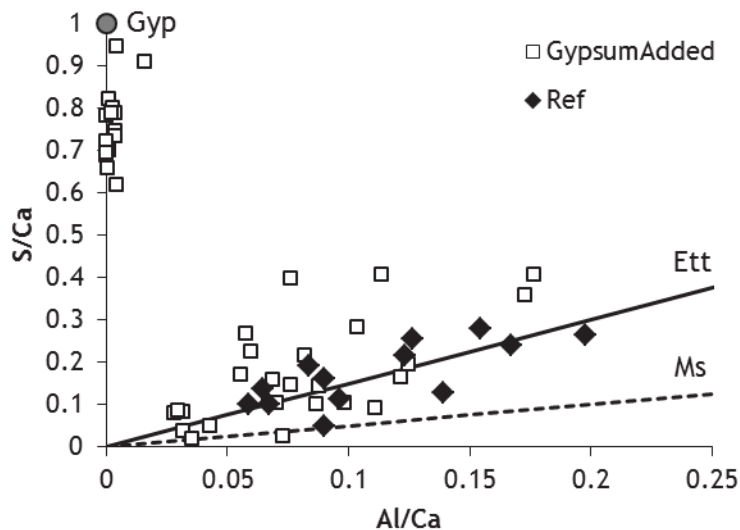
283 The chemical composition of the cement matrix in both gypsum-contaminated and gypsum-free
284 28 days hydrated floor screeds was investigated by EDS microanalysis. Points were selected within
285 the cement matrix to verify the S content, and for the gypsum contaminated samples, within the
286 (former) gypsum grains to check for formation of cement hydrate phase. Figure 6 shows the EDS
287 results in a S/Ca vs Al/Ca plot. This plot enables to distinguish between sulfur bearing phases such as
288 gypsum, ettringite and monosulfate. In the reference sample the EDS results scatter around the trend
289 lines between C-S-H and regular cement hydrates such as ettringite and monosulfate. In the gypsum
290 contaminated samples, the EDS points taken in the cement matrix are shifted upwards to higher S/Ca
291 levels, indicating a change in the hydrate assemblage towards the co-occurrence of ettringite and
292 gypsum.

293

294 The thermodynamic modelling results in section 3.2.2 indicate that this shift coincides with a
295 strong increase in sulfate concentrations in solution and excessive leaching. The EDS point analyses
296 taken within the gypsum particles do not show the presence of cement hydrates containing either
297 aluminates or silicates. This is to be expected since sulfate is (much) more soluble than either
298 aluminate or silicate. Sulfate thus diffuses out from the gypsum particles into the cement matrix.
299



300
301 Figure 5. Electron microscopy images of floor screeds made with crushed AAC demolition waste and mixed
302 C&DW mixed recycled aggregates. The floor screeds contained gypsum impurities and were found to exceed
303 sulfate leaching regulations. a) Overview image showing large pores (P) and an unreacted gypsum grain (G)
304 embedded in the floor screed matrix. b) Close-up on AAC aggregate grain, gypsum crystals enclosed within the
305 AAC are marked. c) Gypsum grain indicated in a). d) S element mapping of the area in c).
306



307

308 Figure 6. EDS point analyses plotted as S/Ca vs. Al/Ca for a reference floor screed made containing no gypsum
 309 particles and a floor screed mix in which gypsum particles were identified and sulfate leaching was off-limits (cf.
 310 Fig. 5). Both samples were cured for 28 days. Average S/Ca ratios of the cement matrix were higher in the
 311 gypsum (Gyp) containing samples indicating a shift in the hydrate assemblage from monosulfate (Ms) +
 312 ettringite (Ett) to Ett+Gyp.

313 4 Conclusions

314 This research shows that AAC demolition waste can be recycled as fine aggregate (0-8 mm) in
 315 floor screed formulations, creating a new valorisation route for a waste stream that currently still is
 316 being landfilled. The reaction of the cement binder with the soluble sulfate from the AAC waste
 317 caused the formation of insoluble ettringite, hereby strongly reducing sulfate leaching. Two conditions
 318 are crucial for a secure sulfate immobilisation, namely high pH conditions (>12) and very low gypsum
 319 levels contamination in the recycled AAC waste.

320 The pH dependency of sulfate leaching is in line with the modelled ettringite solubility.
 321 Sufficiently high pH conditions can be obtained by the use of CEM I. Blended cements show a lower
 322 pH buffering capacity due to the occurrence of pozzolanic reactions.

323

324 When the AAC waste is contaminated with gypsum (e.g. from plasterboards), the immobilization
 325 capacity by ettringite formation can become exhausted. These observations from leaching experiments

326 are confirmed by thermodynamic modelling and SEM analysis (EDS and multispectral element
327 mappings) of the microstructure.

328 As a final conclusion, with the use of CEM I and a good acceptance policy of AAC waste, it is
329 possible to successfully recycle AAC demolition waste in a high-grade construction product.

330

331 **Acknowledgements**

332 The authors express their gratitude to the EU FP7 project IRCOW (Innovative Strategies for High-
333 Grade Material Recovery from Construction and Demolition Waste - grant agreement no. 265212) for
334 funding the research presented in this paper. Further information about the project is accessible at
335 www.ircow.eu.

336

337 **References**

- [1] Narayanan N, Ramamurthy K. Structure and properties of aerated concrete: a review. *Cem Concr Comp* 2000;22:321-9.
- [2] Mitsuda T, Sasaki K, Ishida H. Phase Evolution during Autoclaving Process of Aerated Concrete. *J Am Ceram Soc* 1992;75:1858-63.
- [3] Straube B, Langer P, Stumm A. Durability of autoclaved aerated concrete. In. Conference on Durability of Building Materials and Components. Istanbul, Turkey; 11-14 May, 2008.
- [4] Baltakys K. Influence of gypsum additive on the formation of calcium silicate hydrates in mixtures with C/S = 0.83 or 1.0. *Mater Sci* 2009;27:1091-101.
- [5] Sakiyama M, Oshio Y, Mitsuda T. Influence of Gypsum on the Hydrothermal Reaction of Lime-Quartz System and on the Strength of Autoclaved Calcium Silicate Product. *Inorg Mater* 2000;7:685-91.
- [6] Cox J, Sizaire J, Meulders P, Van Overmeire E, Ingelaere A. *Le Béton Cellulaire - Matériau d'Avenir*. Brussels: Febecel; 2007.

- [7] Lang-Beddoe I, Schober G. Wiederverwertung von Porenbeton - Untersuchungsergebnisse zur Umweltverträglichkeit. *Baust Recycl Deponietechn* 1999;15:4-8.
- [8] Brocken H, Nijland TG. White efflorescence on brick masonry and concrete masonry blocks, with special emphasis on sulfate efflorescence on concrete blocks. *Constr Build Mater* 2004;18:315-23.
- [9] Müllauer W, Beddoe RE, Heinz D. Sulfate attack expansion mechanisms. *Cem Concr Res* 2013;52:208-15.
- [10] Santhanam M, Cohen M, Olek J. Sulfate attack research - whither now? *Cem Concr Res* 2001;31:845-51.
- [11] Geurts JJM, Sarneel JM, Willers BJC, Roelofs JGM, Verhoeven JTA, Lamers LPM. Interacting effects of sulphate pollution, sulphide toxicity and eutrophication on vegetation development in fens: A mesocosm experiment. *Environ Pollut* 2009;157:2072-81.
- [12] Nielsen P, Vrijders J, Broos K, Quaghebeur M. Recycling of autoclaved aerated concrete In 8th International conference on Sustainable management of waste and recycled materials in construction. Gothenburg, Sweden, 30 May - 1 June, 2012.
- [13] Zaetang Y, Wongsa A, Sata V, Chindaprasirt P. Use of lightweight aggregates in pervious concrete. *Constr Build Mater* 2013;48:585-91.
- [14] Schoon J, De Buysser K, Van Driessche I, De Belie N. Feasibility study on the use of cellular concrete as alternative raw material for Portland clinker production. *Constr Build Mater* 2013;48:725-33.
- [15] Karczmarczyk A, Baryla A, Bus A. Effect of P-Reactive Drainage Aggregates on Green Roof Runoff Quality. *Water* 2014;6:2575-89.
- [16] Brouwer JP, Mulder E, Frénay J, Blaakmeer J, van Opstal C. Use of sulphate containing sieve sands in building materials. *Waste Manag Ser* 2000;1:402-10.

- [17] Minard H, Garrault S, Regnaud L, Nonat A. Mechanisms and parameters controlling the tricalcium aluminate reactivity in the presence of gypsum. *Cem Concr Res* 2007;37:1418-26.
- [18] Quennoz A, Scrivener KL. Hydration of C3A-gypsum systems. *Cem Concr Res* 2012;42:1032-41.
- [19] Nicoleau L, Schreiner E, Nonat A. Ion-specific effects influencing the dissolution of tricalcium silicate. *Cem Concr Res* 2014;59:118-38.
- [20] Ambroise J, Péra J. Immobilization of calcium sulfate contained in demolition waste. *J Hazard Mater* 2008;151:840-6.
- [21] Péra J, Ambroise J. New applications of calcium sulfoaluminate cement. *Cem Concr Res* 2004;34:671-6.
- [22] Winnefeld F, Barlag S. Influence of calcium sulfate and calcium hydroxide on the hydration of calcium sulfoaluminate clinker. *ZKG Int* 2009;62:42-53.
- [23] Hargis CW, Kirchheim AP, Monteiro PJM, Gartner EM. Early age hydration of calcium sulfoaluminate (synthetic ye'elimite, C4A3S) in the presence of gypsum and varying amounts of calcium hydroxide. *Cem Concr Res* 2013;48:105-15.
- [24] Bizzozero J, Gosselin C, Scrivener KL. Expansion mechanisms in calcium aluminate and sulfoaluminate systems with calcium sulfate. *Cem Concr Res* 2014;56:190-202.
- [25] Regeling Bodemkwaliteit. Bijlage A: Maximale samenstellings- en emissiewaarden bouwstoffen.
- [26] Thoenen T, Hummel W, Berner U, Curti E. The PSI/Nagra Chemical Thermodynamic Database 12/07. Villingen: Paul Scherrer Institut; 2014.
- [27] Kulik DA. Improving the structural consistency of CSH solid solution thermodynamic models. *Cem Concr Res* 2011;41:477-95.
- [28] Lothenbach B, Matschei T, Möschner G, Glasser FP. Thermodynamic modelling of the effect of temperature on the hydration and porosity of Portland Cement. *Cem Concr Res* 2008;38:1-18.

- [29] Vollpracht A, Snellings R, Lothenbach B. The pore solution of blended cements: a review. *Subm to Mat Struct* 2015.
- [30] Screening van de milieuhygiënische kwaliteit en kwaliteitsopvolging van puingranulaten. Mechelen: OVAM; 2006.
- [31] Vrancken KC, Laethem B. Recycling options for Gypsum from Construction and Demolition Waste. *Waste Manag Ser* 2000;1:325-31.
- [32] Lothenbach B, Scrivener K, Hooton RD. Supplementary cementitious materials. *Cem Concr Res* 2011;41:1244-56.
- [33] De Weerd K, Haha M Ben, Le Saout G, Kjellsen KO, Justnes H, Lothenbach B. Hydration Mechanisms of ternary Portland cements containing limestone powder and fly ash. *Cem Concr Res* 2011;41:279-91.
- [34] Matschei T, Glasser FP. Buffering in cementitious systems based on OPC. 13th Int. Congr. Chem. Cem., 2011, p. 1-7.
- [35] Divet L, Randriambololona R. Delayed ettringite formation: The effect of temperature and basicity on the interaction of sulphate and CSH phase. *Cem Concr Res* 1998;28:357-63.